Inert Doublet Dark Matter with an additional scalar singlet and 125 GeV Higgs Boson

Amit Dutta Banik [1], **Debasish Majumdar** [2]

Astroparticle Physics and Cosmology Division,
Saha Institute of Nuclear Physics,
1/AF Bidhannagar, Kolkata 700064, India

arXiv:1404.5840v1 [hep-ph] 23 Apr 2014

Abstract

In this work we consider a model for particle dark matter where an extra inert Higgs doublet and an additional scalar singlet is added to the Standard Model (SM) Lagrangian. The dark matter candidate is obtained from only the inert doublet. The stability of this one component dark matter is ensured by imposing a Z_2 symmetry on this additional inert doublet. The additional singlet scalar has a vacuum expectation value (VEV) and mixes with the Standard Model Higgs doublet resulting in two CP even scalars h_1 and h_2. We treat one of these scalars, h_1, to be consistent with the SM Higgs like boson of mass around 125 GeV reported by the LHC experiment. These two CP even scalars affect the annihilation cross-section of this inert doublet dark matter resulting in a larger dark matter mass region that satisfies the observed relic density. We also investigate the $h_1 \to \gamma\gamma$ and $h_1 \to \gamma Z$ processes and compared these with LHC results. This is also used to constrain the dark matter parameter space in the present model. We find that the dark matter candidate in the mass region $\frac{m_1}{2} < m_H < m_W$ GeV ($m_1 = 125$ GeV, mass of h_1) satisfies the recent bound from LUX direct detection experiment.

[1]email: amit.duttabanik@saha.ac.in
[2]email: debasish.majumdar@saha.ac.in

1 Introduction

Existence of a newly found Higgs-like scalar boson of mass about 125 GeV has been reported by recent LHC results. ATLAS [1] and CMS [2] independently confirmed the discovery of a new scalars and measured signal strengths of the Higgs-like scalar to various decay channels separately. ATLAS has reported a Higgs to di-photon signal strength ($R_{\gamma\gamma}$) about $1.65^{+0.34}_{-0.30}$ [3]. On the other hand Higgs to di-photon signal strength evaluated by CMS experiment is found to be about $0.78^{+0.28}_{-0.26}$ [4]. Despite the success of Standard Model (SM) of particle physics, it fails to produce a plausible explanation of dark matter (DM) in modern cosmology. Existence of dark matter is firmly established by the observations of galaxy rotation curves and analysis of cosmic microwave background (CMB) etc. DM relic density predicted by the PLANCK [5] and WMAP [6] results suggest that about 26.5% of our Universe is constituted by DM. The particle constituent of dark matter is still unknown and SM of particle physics appears inadequate to address the issues regarding dark matter. The observed dark matter relic density reported by CMB anisotropy probes suggests that weakly interacting massive particle or WIMP [7, 8]. or WIMP can be assumed to serve as a feasible candidate for dark matter. Thus, in order to propose a feasible candidate for dark matter one sould invoke a theory beyond SM and in this regard simple extension of SM scalar or fermion sector or both could be of interest in respect of addressing the problem of a viable candidate of dark matter and dark matter physics. There are other theories though beyond Standard Model (BSM) such as the elegant theory of Supersymmetry (SUSY) in which the dark matter candidate is supposedly the LSP or lightest SUSY particle formed by the superposition of neutral gauge bosons and Higgs boson [9]. Extra dimension models [10] providing Kaluza-Klein dark matter candidates are also explored at length in literature. Comprehensive studies on simplest extension of SM with additional scalar singlet where a discrete Z_2 symmetry stabilizes the scalar is studied elaborately in earlier works such as [11]-[22]. It is also demonstrated by previous authors that singlet fermion extension of SM can also be a viable candidate of dark matter [23]-[25]. SM extensions with two Higgs doublets and a singlet are also addressed earlier where the additional singlet is the proposed of dark matter candidate [26, 27]. Among various extensions of SM, a simplest model is to introduce an additional SU(2) scalar doublet which produces no VEV. The resulting model namely Inert Doublet Model (IDM) provides a viable explanation for DM. Satbility of this inert doublet ensured by a discrete Z_2 symmetry and the lightest inert particle (LIP) in this theory can be assumed to be a plausible DM candidate. Phenomenology of IDM has been elaborately studied in literatures [28]-[37]. In the present work, we consider a two Higgs doublet model (THDM) with an additional scalar singlet, where one of the Higgs doublet is identical to the inert doublet, i.e., one of the doublet assumes no VEV and all the SM sector including the newly added singlet are even under an imposed discrete symmetry (Z_2) while the inert doublet is odd uner that Z_2 symmetry. Since inert scalars do not interact with SM particles, are stable and LIP is considered as a potential DM candidate. Presence of an additional singlet scalar enriches the phenomenology of Higgs sector and DM sector.

Various ongoing direct detection experiments such as XENON100 [38], LUX [39], CDMS [40] etc.

provide upper limits on dark matter-nucleon scattering cross sections for different possible dark matter mass. The CDMS [40] experiment also claimed to have observed three potential signals of dark matter at low mass region ($\sim$ 8 GeV). Direct detection experiments such as DAMA [41], CoGeNT [42] and CRESST [43] also provide bounds on dark matter-nucleon scattering cross sections for different dark matter masses. These experiments predict the presence of low mass dark matter candidate that contradict with XENON100 or LUX results since they provide a much lower bound for dark matter-nucleon scattering cross section. We also test our model by calculating the $R_{\gamma\gamma}$ for $h \to \gamma\gamma$ signal and comparing the same with those given by LHC experiment.

In this work, we consider an Inert Doublet Model (IDM) along with an additional singlet scalar field S. A discrete Z_2 symmetry, under which all SM particles along with the singlet scalar S are even while the inert doublet considered is odd, allows the LIP (H) to remain stable and serve as a viable dark matter candidate. Additional scalar singlet having a non zero VEV mixes with the SM Higgs, provides two CP even Higgs states. We consider one of the scalars, h_1, to be the SM-like Higgs. Then h_1 should be compatible with SM Higgs and one can compare the relevant calculations for h_1 with that obtained in LHC experiment. The model parameter space is first constrained by theoretical conditions such as vacuum stability, perturbativity, unitarity and then by the relic density bound given by PLANCK/WMAP experiments. We evaluate the direct detection scattering cross-section $\sigma_{\rm SI}$ with the resulting constrained parameters for different LIP masses m_H and investigate the regions in $\sigma_{\rm SI} - m_H$ plane that satisfy the bounds from experiments like LUX, XENON etc. We also calculate the signal strength $R_{\gamma\gamma}$ for $h_1 \to \gamma\gamma$ channel in the present framework and compare them with the experimentally obtained limits for this quantity from CMS and ATLAS experiments. This will further constrain the model parameter space. We thus obtain regions in $\sigma_{\rm SI} - m_H$ plane in the present framework that satisfy not only the experimental results for dark matter relic density and scattering cross-sections but compatible with LHC results too.

The paper is organised as follows. In Sec. 2 we present a description of the model and model parameters with relevant bounds from theory (vacuum stability, pertubativity and unitarity) and experiments (PLANCK/WMAP, direct detection experiments, LHC etc.). In Sec. 3 we describe the relic density and annihilation cross section measurements for dark matter and modified $R_{\gamma\gamma}$ and $R_{\gamma Z}$ processes due to inert charged scalars. We constrain the model parameter space satisfying the relic density requirements of dark matter and present the correlation between $R_{\gamma\gamma}$ and $R_{\gamma Z}$ processes in Section 4. In Sec. 5, we further constrain the results by direct detection bounds on dark matter. Finally, in Sec. 6 we summarize the work briefly with concluding remarks.

2 The Model

2.1 Scalar Sector

In our model we add an additional SU(2) scalar doublet and a a real scalar singlet S. Similar to the widely studied inert doublet model or IDM where the added SU(2) scalar doublet to the SM Lagrangian

is made "inert" (by imposing a Z_2 symmetry that ensures no interaction with SM fermions and the inert doublet does not generate any vev), here too the extra doublet is assumed to be odd under a discrete Z_2 symmetry (IDM). Under this Z_2 symmetry however, all SM particles as also the added singlet S remain unchanged. The potential is expressed as

$$\begin{aligned} V &= m_{11}^2 {\Phi_1}^\dagger \Phi_1 + m_{22}^2 {\Phi_2}^\dagger \Phi_2 + \frac{1}{2} m_s^2 S^2 + \lambda_1 ({\Phi_1}^\dagger \Phi_1)^2 + \lambda_2 ({\Phi_2}^\dagger \Phi_2)^2 + \lambda_3 (\Phi_1^\dagger \Phi_1)(\Phi_2^\dagger \Phi_2) \\ &+ \lambda_4 (\Phi_2^\dagger \Phi_1)(\Phi_1^\dagger \Phi_2) + \frac{1}{2}\lambda_5 [(\Phi_2^\dagger \Phi_1)^2 + (\Phi_1^\dagger \Phi_2)^2] + \rho_1 (\Phi_1^\dagger \Phi_1) S + \rho_1' (\Phi_2^\dagger \Phi_2) S \\ &+ \rho_2 S^2 (\Phi_1^\dagger \Phi_1) + \rho_2' S^2 (\Phi_2^\dagger \Phi_2) + \frac{1}{3}\rho_3 S^3 + \frac{1}{4}\rho_4 S^4, \end{aligned} \tag{1}$$

where $m_k (k = 11, 22, s)$ etc. and all the coupling parameters (λ_i, ρ_i, ${\rho'}_i$, $i = 1, 2, 3, ...$ etc.) are assumed to be real. In Eq. 1, Φ_1 is the ordinary SM Higgs doublet and Φ_2 is the inert Higgs doublet. After spontaneous symmetry breaking Φ_1 and S acquires VEV and expressed as

$$\Phi_1 = \begin{pmatrix} 0 \\ \frac{1}{\sqrt{2}}(v+h) \end{pmatrix}, \qquad \Phi_2 = \begin{pmatrix} H^+ \\ \frac{1}{\sqrt{2}}(H+iA) \end{pmatrix}, \qquad S = v_s + s\,. \tag{2}$$

In the above v_s denotes the VEV of the field S and s is the real singlet scalar. Relation among model parameters can be obtained from the extremum conditions of the potenial expressed in Eq. 1 and are given as

$$\begin{aligned} m_{11}^2 + \lambda_1 v^2 + \rho_1 v_s + \rho_2 v_s^2 = 0\,, \\ m_s^2 + \rho_3 v_s + \rho_4 v_s^2 + \frac{\rho_1 v^2}{2 v_s} + \rho_2 v^2 = 0\,. \end{aligned}$$

Mass terms of various scalar particles as derived from the potential are

$$\begin{aligned} \mu_h^2 &= 2\lambda_1 v^2 \\ \mu_s^2 &= \rho_3 v_s + 2\rho_4 v_s^2 - \frac{\rho_1 v^2}{2 v_s} \\ \mu_{hs}^2 &= (\rho_1 + 2\rho_2 v_s) v \\ m_{H^\pm}^2 &= m_{22}^2 + \lambda_3 \frac{v^2}{2} + \rho_1' v_s + \rho_2' v_s^2 \\ m_H^2 &= m_{22}^2 + (\lambda_3 + \lambda_4 + \lambda_5)\frac{v^2}{2} + \rho_1' v_s + \rho_2' v_s^2 \\ m_A^2 &= m_{22}^2 + (\lambda_3 + \lambda_4 - \lambda_5)\frac{v^2}{2} + \rho_1' v_s + \rho_2' v_s^2\ . \end{aligned} \tag{3}$$

The mass eigenstates h_1 and h_2 are linear combinations of h and s and can be written as

$$\begin{aligned} h_1 = s\ \sin\alpha + h\ \cos\alpha\,, \\ h_2 = s\ \cos\alpha - h\ \sin\alpha\,, \end{aligned} \tag{4}$$

α being the mixing angle between h_1 and h_2, is given by

$$\tan\alpha \equiv \frac{x}{1+\sqrt{1+x^2}}\,, \tag{5}$$

where $x = \frac{2\mu_{hs}^2}{(\mu_h^2-\mu_s^2)}$. Masses of the physical neutral scalars h_1 and h_2 are

$$m_{1,2}^2 = \frac{\mu_h^2+\mu_s^2}{2} \pm \frac{\mu_h^2-\mu_s^2}{2}\sqrt{1+x^2}. \tag{6}$$

We consider h_1 with mass $m_1 = 125$ GeV as the SM-like Higgs boson and the mass of the other scalar h_2 in the model is denoted as m_2 with $m_2 > m_1$. Couplings of the physical scalars h_1 and h_2 with SM particles are modified by the factors $\cos\alpha$ and $\sin\alpha$ respectively. In the present framework H and A are stable as long as the Z_2 symmetry is unbroken and hence these neutral scalars can be viable candidates for dark matter. Here, the coupling λ_5 serves as a mass splitting factor between H and A. We consider H to be the lightest inert particle (LIP) which is stable and is DM candidate in this work. We take $\lambda_5 < 0$ in order to make H to be the lightest stable inert particle. In the present framework, both the scalars h_1 and h_2 couple with the lightest inert particle H. Couplings of the scalar bosons (h_1 and h_2) with the inert dark matter H are given by

$$\begin{aligned}
\lambda_{h_1HH}v &= \left(\frac{\lambda_{345}}{2}c_\alpha - \frac{\lambda_s}{2}s_\alpha\right)v\,,\\
\lambda_{h_2HH}v &= \left(\frac{\lambda_{345}}{2}s_\alpha + \frac{\lambda_s}{2}c_\alpha\right)v
\end{aligned} \tag{7}$$

where $\lambda_{345} = \lambda_3+\lambda_4+\lambda_5$, $\lambda_s = \frac{\rho_1'+2\rho_2'v_s}{v}$ and $s_\alpha(c_\alpha)$ denotes $\sin\alpha(\cos\alpha)$. Couplings of scalar bosons with charged scalars $H^\pm$ are

$$\begin{aligned}
\lambda_{h_1H^+H^-}v &= (\lambda_3 c_\alpha - \lambda_s s_\alpha)\,v\,,\\
\lambda_{h_2H^+H^-}v &= (\lambda_3 s_\alpha + \lambda_s c_\alpha)\,v.
\end{aligned} \tag{8}$$

2.2 Constraints

The model parameters are bounded by theoretical and experimental constraints.

- **Vacuum Stability** - Vacuum stability constraints requires the potential to remain bounded from below. Conditions for the stability of the vacuum are

$$\begin{aligned}
\lambda_1,\,\lambda_2,\,\rho_4 &> 0\,,\\
\lambda_3 + 2\sqrt{\lambda_1\lambda_2} &> 0\,,\\
\lambda_3+\lambda_4+\lambda_5 + 2\sqrt{\lambda_1\lambda_2} &> 0\,,\\
\rho_2 + \sqrt{\lambda_1\rho_4} &> 0\,,\\
\rho_2' + \sqrt{\lambda_2\rho_4} &> 0\,.
\end{aligned} \tag{9}$$

- **Pertubativity** - For a theory to be acceptable in perturbative limits, we have to constrain high energy quartic interactions at tree level. The eigenvalues $|\Lambda_i|$ of quartic couplings (scattering) matrix must be smaller than 4π.

- **LEP** LEP[44] results constrains the Z boson decay width and masses of scalar particles

$$\begin{aligned} m_H + m_A &> m_Z \ , \\ m_{H^\pm} &> 79.3 \text{ GeV}. \end{aligned} \tag{10}$$

- **Relic Density** - Parameter space is also constrained by the measurement of relic density of dark matter candidate. Relic density of the lightest inert particle (LIP) serving as a viable candidate for dark matter in the present model must satisfy PLANCK/WMAP results,

$$\Omega_{\rm DM} h^2 = 0.1199 \pm 0.0027 \ . \tag{11}$$

- **Higgs to Diphoton Rate $\mathbf{R}_{\gamma\gamma}$** Bound on Higgs to two photon channel has been obtained from experiments performed by LHC. The reported singal strength for the Higgs to diphoton channel from ATLAS and CMS are given as

$$R_{\gamma\gamma}|_{\rm ATLAS} = 1.65^{+0.34}_{-0.30} \, , R_{\gamma\gamma}|_{\rm CMS} = 0.78^{+0.28}_{-0.26} \ .$$

- **Direct Detection Experiments** - The bounds on dark matter from direct detection experiments are based on the elastic scattering of the dark matter particle off a scattering nucleus. Dark matter direct detection experiments set constraints on the dark matter - nucleus (nucleon) elastic scattering cross section. Limits on scattering cross sections for different dark matter mass cause further restrictions on the model parameters. Experiments like CDMS, DAMA, CoGeNT, CRESST etc. provide effective bounds on low mass dark matter. Stringent bounds on midddle mass and high mass dark matter are obtained from XENON100 and LUX experiments.

3 Dark matter

3.1 Relic density

Relic density of dark matter is constrained by the results of PLANCK and WMAP. Dark matter relic abundance for the model is evaluated by solving the evolution of Boltzmann equation given as [45]

$$\frac{{\rm d}n_H}{{\rm d}t} + 3{\rm H}n_H \quad = \quad -\langle\sigma{\rm v}\rangle(n_H^2 - n_{H{\rm eq}}^2) \ . \tag{12}$$

In Eq. 12, $n_H(n_{Heq})$ denotes the number density (equilibrium number density) of dark matter H and H is the Hubble constant. In Eq. 12, $\langle\sigma{\rm v}\rangle$ denotes the thermal averaged annihilation cross section of

dark matter particle to SM species. The dark matter relic density can be obtained by solving Eq. 12 and is written as

$$\Omega_{\rm DM}{\rm h}^2 \;=\; \frac{1.07\times 10^9 x_F}{\sqrt{g_*}M_{\rm Pl}\langle\sigma{\rm v}\rangle}\,. \tag{13}$$

In the above, $M_{\rm Pl} = 1.22\times 10^{19}$GeV, is the Planck scale mass whereas g_* is the effective number of degrees of freedom in thermal equilibrium and h is the Hubble parameter in unit of 100 km s^{-1}Mpc^{-1}. In Eq. 13, $x_F = M/T_F$, where T_F is the freeze out temperature of the annihilating particle and M is the mass of the dark matter (m_H for the present scenario). Freeze out temperature T_F for the dark matter is obtained from the iterative solution to the equation

$$x_F \;=\; \ln\left(\frac{M}{2\pi^3}\sqrt{\frac{45M_{\rm Pl}^2}{2g_*x_F}}\langle\sigma{\rm v}\rangle\right)\,. \tag{14}$$

3.2 Annihilation cross section

Annihilation of inert dark matter H to SM particles is governed by processes involving scalar (h_1, h_2) mediated s($\simeq 4m_H^2$) channels. Thermal averaged annihilation cross section $\langle\sigma{\rm v}\rangle$ of dark matter H to SM fermions are given as

$$\langle\sigma{\rm v}_{HH\to f\bar{f}}\rangle \;=\; n_c\frac{m_f^2}{\pi}\beta_f^3\left|\frac{\lambda_{h_1HH}\cos\alpha}{4m_H^2-m_1^2+i\Gamma_1m_1}+\frac{\lambda_{h_2HH}\sin\alpha}{4m_H^2-m_2^2+i\Gamma_2m_2}\right|^2\,. \tag{15}$$

In the above, m_x represents mass of the particle $x(\equiv f,\ H$ etc.), n_c is the colour quantum number (3 for quarks and 1 for leptons) with $\beta_a = \sqrt{1-\frac{m_a^2}{m_H^2}}$ and $\Gamma_i(i=1,2)$ denotes the total decay width of each of the two scalars h_1 and h_2. For DM mass $m_H > (m_W, m_Z)$, annihilation of DM to gauge boson (W or Z) channels will yield high annihilation cross-section. Since $\Omega_{\rm DM}\sim\langle\sigma{\rm v}\rangle^{-1}$ (Eq. 13), the relic density for the dark matter with mass $m_H > m_W$ or m_Z in the present model in fact falls below the relic density given by WMAP or PLANCK as the four point interaction channel $HH\to W^+W^-$or ZZ will be accessible and as a result increase in total annihilation cross-section will be observed. Thus the possibility of a single component DM in the present framework is excluded for mass $m_H > m_W,\ m_Z$ [3]. Higgs like boson h_1 and the scalar h_2 may also decay to dark matter candidate H when the condition $m_H < m_i/2(i=1,2)$ is satisfied. Contributions of invisible decay widths of h_1 and h_2 are taken into account when the condition $m_H < m_i/2(i=1,2)$ is satisfied. Invisible decay width is represented by the relation

$$\Gamma_{inv}(h_i\to 2H) = \frac{\lambda_{h_iHH}^2v^2}{16\pi m_i}\sqrt{1-\frac{4m_H^2}{m_i^2}}\,. \tag{16}$$

[3]Similar results for IDM are also obtained in previous work (Ref. [51]) where a two component dark matter was considered in order to circumvent this problem.

3.3 Modification of $R_{\gamma\gamma}$ and $R_{\gamma Z}$

Recent studies of IDM [46, 47, 48] and two Higgs doublet models [49, 50] have reported that a low mass charged scalar could possibly enhance the $h_1 \to \gamma\gamma$ signal strength $R_{\gamma\gamma}$. Correlation of $R_{\gamma\gamma}$ with $R_{\gamma Z}$ is also accounted for as well [47, 50]. The quantities $R_{\gamma\gamma}$ and $R_{\gamma Z}$ are expressed as

$$R_{\gamma\gamma} = \frac{\sigma(pp \to h_1)}{\sigma(pp \to h)^{\rm SM}} \frac{Br(h_1 \to \gamma\gamma)}{Br(h \to \gamma\gamma)^{\rm SM}} \tag{17}$$

$$R_{\gamma Z} = \frac{\sigma(pp \to h_1)}{\sigma(pp \to h)^{\rm SM}} \frac{Br(h_1 \to \gamma Z)}{Br(h \to \gamma Z)^{\rm SM}} \ , \tag{18}$$

where σ is the Higgs production cross section and Br represents the branching ratio of Higgs to final states. Branching ratio to any final state is given by the ratio of partial decay width for the particular channel to the total decay width of decaying particle. For IDM with additional singlet scalar, the ratio $\frac{\sigma(pp\to h_1)}{\sigma(pp\to h)^{\rm SM}}$ in Eqs. 17-18 is represented by a factor $\cos^2\alpha$. Standard Model branching ratios $Br(h \to \gamma\gamma)^{\rm SM}$ and $Br(h \to \gamma Z)^{\rm SM}$ for a 125 GeV Higgs boson is 2.28×10^{-3} and 1.54×10^{-3} respectively [52]. To evaluate the branching ratios $Br(h_1 \to \gamma\gamma)$ and $Br(h_1 \to \gamma Z)$, we compute the total decay width of h_1. Invisible decay of h_1 to dark matter particle H is also taken into account and evaluated using Eq. 16 when the condition $m_H < m_1/2$ is satisfied. Partial decay widths $\Gamma(h_1 \to \gamma\gamma)$ and $\Gamma(h_1 \to \gamma Z)$ according to the model are given as

$$\begin{aligned}
\Gamma(h_1 \to \gamma\gamma) &= \frac{G_F \alpha_s^2 m_1^3}{128\sqrt{2}\pi^3} \left| \cos\alpha \left(\frac{4}{3} F_{1/2}\left(\frac{4m_t^2}{m_1^2}\right) + F_1\left(\frac{4m_W^2}{m_1^2}\right)\right) + \frac{\lambda_{h_1 H^+ H^-} v^2}{2m_{H^\pm}^2} F_0\left(\frac{4m_{H^\pm}^2}{m_1^2}\right)\right|^2 , \\
\Gamma(h_1 \to \gamma Z) &= \frac{G_F^2 \alpha_s}{64\pi^4} m_W^2 m_1^3 \left(1 - \frac{m_Z^2}{m_1^2}\right)^3 \left| -2\cos\alpha \frac{1 - \frac{8}{3}s_W^2}{c_W} F'_{1/2}\left(\frac{4m_t^2}{m_1^2}, \frac{4m_t^2}{m_Z^2}\right)\right. \\
&\quad \left. - \cos\alpha F'_1\left(\frac{4m_W^2}{m_1^2}, \frac{4m_W^2}{m_Z^2}\right) + \frac{\lambda_{h_1 H^+ H^-} v^2}{2m_{H^\pm}^2} \frac{(1 - 2s_W^2)}{c_W} I_1\left(\frac{4m_{H^\pm}^2}{m_1^2}, \frac{4m_{H^\pm}^2}{m_Z^2}\right)\right|^2 ,
\end{aligned} \tag{19}$$

where G_F is the Fermi constant, m_x denotes the mass of particle $x (x \equiv 1, W, Z, t, H^\pm)$ etc. and $s_W (c_W)$ represents $\sin\theta_W (\cos\theta_W)$, θ_W being the weak mixing angle. Expressions for various loop factors ($F_{1/2}$, F_1, F_0, $F'_{1/2}$, F'_1 and I_1) appeared in Eq. 19 are given in Appendix A. It is to be noted that a similar derivation of decay widths and signal strengths ($R'_{\gamma\gamma}$ or $R'_{\gamma Z}$) for the other scalar h_2 can be obtained by replacing m_1, $\cos\alpha$, $\lambda_{h_1 H^+ H^-}$ with m_2, $\sin\alpha$, $\lambda_{h_2 H^+ H^-}$ respectively and this is addressed in Sec. 5.

4 Analysis of $R_{\gamma\gamma}$ and $R_{\gamma Z}$

In this section we compute the quantities $R_{\gamma\gamma}$ and $R_{\gamma Z}$ in the framework of the present model. We restrict the allowed model parameter space for our analysis using the vacuum stability, perturbative unitarity, LEP bounds along with the relic density constraints described in Section 2.2. Dark matter

relic density is evaluated by solving the Boltzmann equation presented in Section 3.1 with the expression for annihilation cross section given in Eq. 15. Model parameters (λ_i, ρ_i), should remain small in order to satisfy perturbative bounds and relic density constraints. Calculations are made for the model parameter limits given below,

$$\begin{aligned} m_1 &= 125 \text{ GeV}\,, \\ 80 \text{ GeV} \leq m_{H^\pm} &\leq 400 \text{ GeV}\,, \\ 0 < m_H &< m_{H^\pm},\ m_A\,, \\ 0 < \alpha &< \pi/2\,, \\ -3 \leq \lambda_3 &\leq 3\,, \\ -3 \leq \lambda_{345} &\leq 3\,, \\ -3 \leq \lambda_s &\leq 3\,. \end{aligned} \tag{20}$$

The couplings λ_{h_1HH} and λ_{h_2HH} (Eq. 7) are required to calculate the scattering cross-section of the dark matter off a target nucleon. Dark matter direct detection experiments are based on this scattering processes whereby the recoil energy of the scattered nucleon is measured. Thus the couplings λ_{h_1HH} and λ_{h_2HH} can be constrained by comparing the computed values of the scattering cross-section for different dark matter masses with those given by different dark matter direct detection experiments. In the present work, $|\lambda_{h_1HH}, \lambda_{h_1H^+H^-}| \leq 3$ is adopted. The following bounds on parameters will also constrain the couplings λ_{h_2HH} and $\lambda_{h_2H^+H^-}$ (Eqs. 7-8). Using Eqs. 12-16 we scan over the parameter space mentioned in Eq. 20 where we also impose the conditions $|\lambda_{h_1H^+H^-},\ \lambda_{h_1HH}| \leq 3$ to calculate the relic densities for the LIP dark matter in the present model. Comparison with the experimentally obtained range of dark matter relic density with the calculated values restricts the allowed model parameter space and gives the range of mass that satisfies observed DM relic density. We have made our calculations for three diffrent values of singlet scalar (h_2) mass namely $m_2 = 140,\ 150$ and 160 GeV. Scanning of the full parameter space yields that for all the cases considered, the limits $-2.1 \leq \lambda_{h_1HH} \leq 1.5$ and $|\lambda_{h_2HH}| \leq 2.0$ are required for satisfying observed DM relic abundance. The condition $|\lambda_{h_1H^+H^-}| \leq 3$ also bounds the coupling $\lambda_{h_2H^+H^-}$. Our calculation reveals that $|\lambda_{h_2H^+H^-}| \leq 4$ is needed in order to satify observed relic density of dark matter. Using the allowed parameter space thus obtained, we measured the signal strengths $R_{\gamma\gamma}$ and $R_{\gamma Z}$ (Eqs. 17-18) by evaluating the corresponding decay widths given in Eq. 19.

In Fig. 1(a-c), shown are the regions in the $R_{\gamma\gamma} - m_H$ plane for the parameter values that satisfy DM relic abundance. As mentioned earler, results are presented for three values of h_2 mass namely $140, 150$ and 160 GeV. Since for low mass DM region, invisible decay channel of h_1 to DM pair remains open, enhancement of $R_{\gamma\gamma}$ is not possible in this regime. $R_{\gamma\gamma}$ becomes greater than unity near the region where $m_H \gtrsim m_2/2$. The region that describe the $R_{\gamma\gamma}$ enhancement is reduced with increasing h_2 mass and thus enhacement is not favoured for higher values of h_2 mass. For the rest of the allowed DM mass parameter space, $R_{\gamma\gamma}$ remains less than 1. The results presented in Fig. 1 indicate that

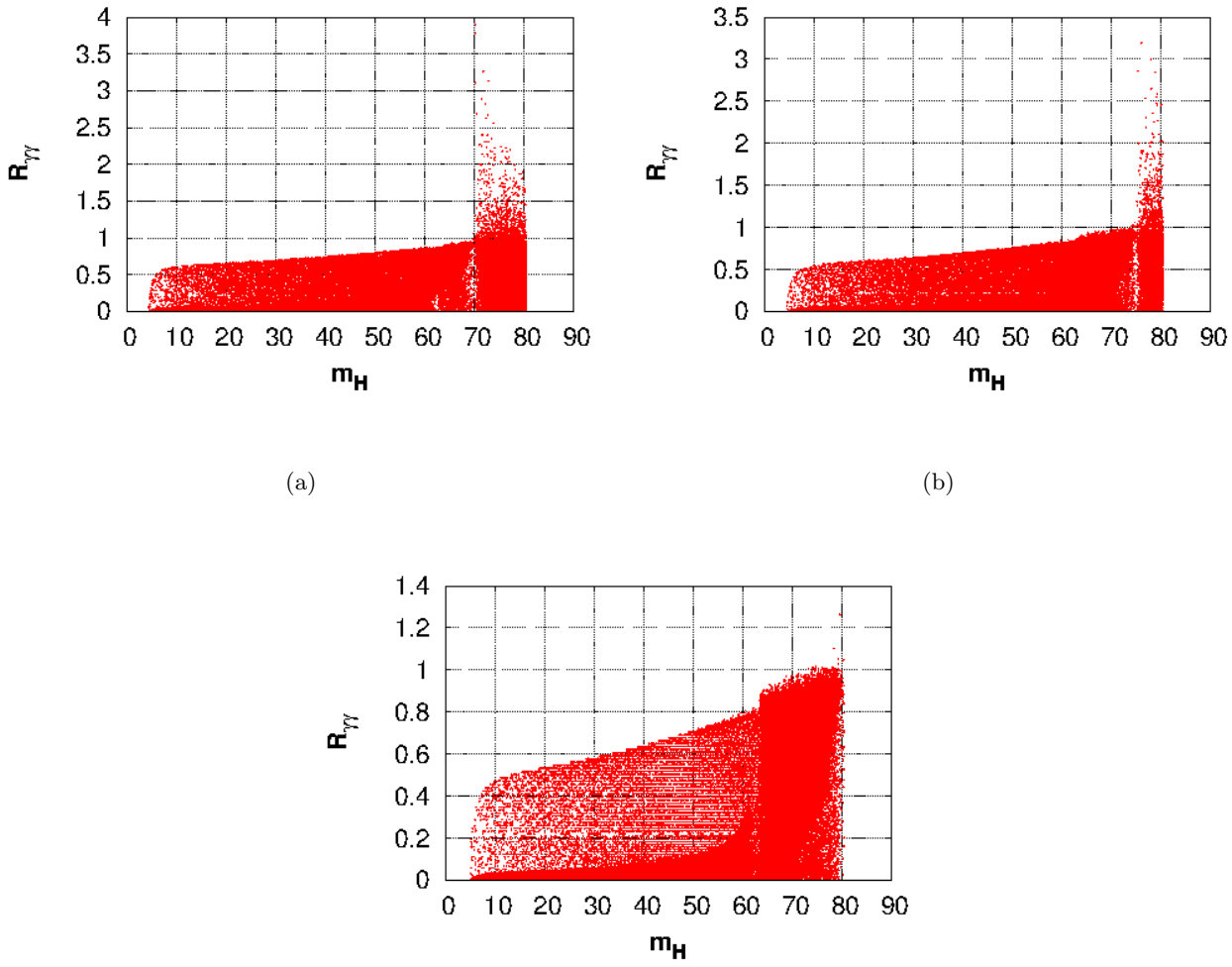

(a) (b)

(c)

Figure 1: Variation of $R_{\gamma\gamma}$ with DM mass m_H satifying DM relic density for $m_2 = 140, 150$ and 160 GeV.

observed enhancement of the $h_1 \to \gamma\gamma$ signal could be a possible indication of the presence of h_2 since $R_{\gamma\gamma} \gtrsim 1$ occurs near the resonance of h_2. The $R_{\gamma\gamma}$ value depends on the coupling $\lambda_{h_1 H^+ H^-}$ and becomes greater than unity only for $\lambda_{h_1 H^+ H^-} < 0$ and interfers constructively with the other loop contributions. Technically, $R_{\gamma\gamma}$ depends on the values of h_2 mass, charged scalar mass $m_{H^\pm}$, coupling $\lambda_{h_1 H^+ H^-}$ and the decay width of invisible decay channel ($\Gamma_{inv}(h_1 \to HH)$). A similar variation for the $h_1 \to \gamma Z$ channel (computed using Eqs. 18-19 and Eq. 20) yields lesser enhancement for $R_{\gamma Z}$ in comparison with $R_{\gamma\gamma}$. This phenomenon can also be verified from the correlation between $R_{\gamma\gamma}$ and $R_{\gamma Z}$. The correlation between the signals $R_{\gamma\gamma}$ and $R_{\gamma Z}$ is shown in Fig. 2a - Fig. 2c for $m_2 = 140, 150, 160$ GeV respectively.

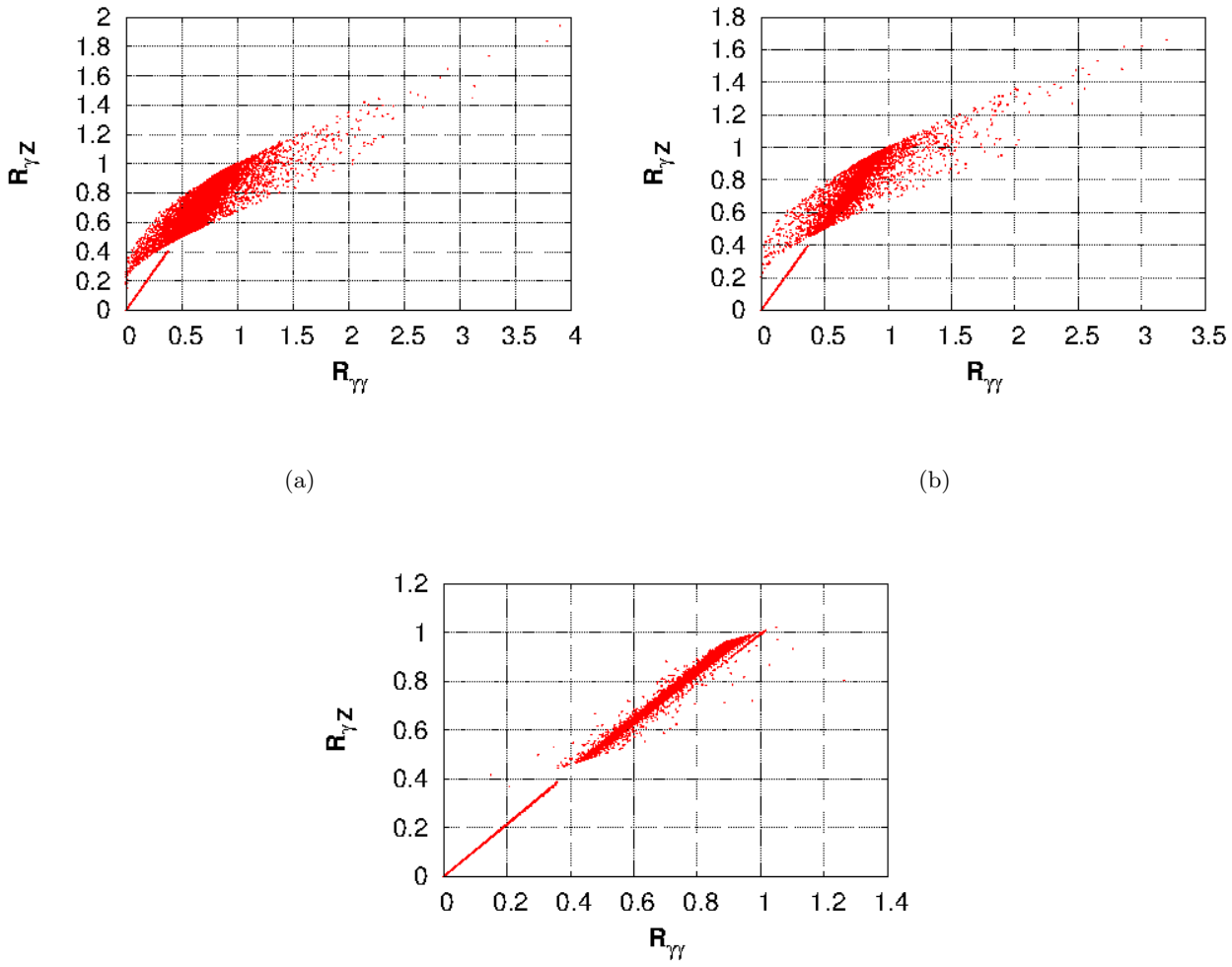

(a)

(b)

(c)

Figure 2: Correlation plots between $R_{\gamma\gamma}$ and $R_{\gamma Z}$ for three choices of h_2 mass (140, 150 and 160 GeV).

Variations of $R_{\gamma\gamma}$ and $R_{\gamma Z}$ satisfy all necessary parameter constraints taken into account inclusive of the relic requirements for DM. In this case (Fig. 2), we further constrain the parameter space of α mentioned in Eq. 20 by imposing the condition $0 < \alpha < \pi/4$. This condition ensures that h_1 is the SM-like Higgs boson [23, 25]. Fig. 2 also indicates that, with increase in the mass (m_2) of h_2, enhancement of $R_{\gamma\gamma}$ and $R_{\gamma Z}$ are likely to reduce. For $m_2 = 140$ GeV, $R_{\gamma\gamma}$ enhances up to four times whereas $R_{\gamma Z}$ increases nearly by a factor 2 with respect to corresponding values predicted SM. On the other hand, for $m_2 = 160$ GeV, $R_{\gamma\gamma}$ varies linearly with $R_{\gamma Z}$ ($R_{\gamma\gamma} \simeq R_{\gamma Z}$) without any significant enhacement. In addition Fig. 2 suggests that for $\cos\alpha \gtrsim 1/\sqrt{2}$, a considerable portion of allowed parameter space with lower values of $R_{\gamma\gamma}$ will disappear. For $|\lambda_{h_1 HH}| < 0.05$, variation of $R_{\gamma\gamma}$ with $R_{\gamma Z}$ is almost linear (with

slope ≈ 1) which is presented by the line passing through origin shown in plots of Fig. 2. The scattered plots represent the correlation for other values of λ_{h_1HH}. For low mass dark matter ($m_H \lesssim m_1/2$), invisible decay channel of h_1 remains open and the processes $h_1 \to \gamma\gamma$ and $h_1 \to \gamma Z$ suffer considerable suppressions. These result in the correlation between the channels $h_1 \to \gamma\gamma$ and $h_1 \to \gamma Z$ to become stronger and $R_{\gamma\gamma}$ *vs* $R_{\gamma Z}$ plot shows more linearity with increase in h_2 mass. For larger h_2 masses, the corresponding charged scalar ($H^{\pm}$) masses for which $R_{\gamma\gamma,\gamma Z} > 1$, tends to increase. Since any increase in $H^{\pm}$ mass will affect the contribution from charged scalar loop, the decay widths $\Gamma(h_1 \to \gamma\gamma, \gamma Z)$ or signal strengths $R_{\gamma\gamma,\gamma Z}$ are likely to reduce. Our numerical results exhibit a positive correlation between the signal strengths $R_{\gamma\gamma}$ and $R_{\gamma Z}$. This is an important feature of the model. Since signal strengths tend to increase with relatively smaller values of m_2, possibility of having a light singlet like scalar is not excluded. The coupling of h_2 with SM sector is suppressed by a factor $\sin\alpha$ which results in a decrease in the signal strengths from h_2 and makes their observations difficult.

5 Direct Detection

Within the framework of our model and allowed values of parameter region obtained in Sec. 4, we calculate spin independent (SI) elastic scattering cross-section for the dark matter candidate in our model off a nucleon in the detector material. We then compare our results with those given by various direct detection experiments and examine the plausibility of our model in explaining the direct detection experimental results. The DM candidate in the present model, interacts with SM via processes led by Higgs exchange. The spin-independent elastic scattering cross section $\sigma_{\rm SI}$ is of the form

$$\sigma_{\rm SI} \simeq \frac{m_r^2}{\pi}\left(\frac{m_N}{m_H}\right)^2 f^2 \left(\frac{\lambda_{h_1HH}\cos\alpha}{m_1^2} + \frac{\lambda_{h_2HH}\sin\alpha}{m_2^2}\right)^2, \tag{21}$$

where m_N and m_H are the masses of scattered nucleon and DM respectively, f represents the scattering factor that depends on pion-nucleon cross-section and quarks involved in the process and $m_r = \frac{m_N m_H}{m_N + m_H}$ is the reduced mass. In the present framework $f = 0.3$ [53] is considered. The computations of $\sigma_{\rm SI}$ for the dark matter candidate in the present model are carried out with those values of the couplings restricted by the experimental value of relic density.

In Fig. 3(a-c), we present the variation of elastic scattering cross section calculated using Eq. 21, with LIP dark matter mass (m_H) for three values of h_2 masses $m_2 = 140, 150$ and 160 GeV. We assume h_1 to be SM-like Higgs and restrict the mixing angle α such that the conditon $\cos\alpha \gtrsim 1/\sqrt{2}$ is satisfied. Also shown in Fig. 3(a-c), superimposed on the computed results, the bounds on $\sigma_{\rm SI}-$ DM mass obtained from DM direct search experiments such as XENON100, LUX, CDMS, CoGeNT, CRESST. From Fig. 3 one notes that in the low mass region, the DM candidate in our model satisfies bounds obtained from experiments like CoGeNT, CDMS, CRESST. We further restrict the $\sigma_{\rm SI} - m_H$ space by identifying in Fig. 3(a-c) the region for which the CMS limit of $R_{\gamma\gamma}$ ($R_{\gamma\gamma} = 0.78^{+0.28}_{-0.26}$) is satisfied. In each of the $\sigma_{\rm SI} - m_H$ plots of Fig. 3(a-c) the light blue region satisfies CMS limit of $R_{\gamma\gamma}$ for three chosen values of m_2. Also marked in black are the specific zones that correspond to the central value of

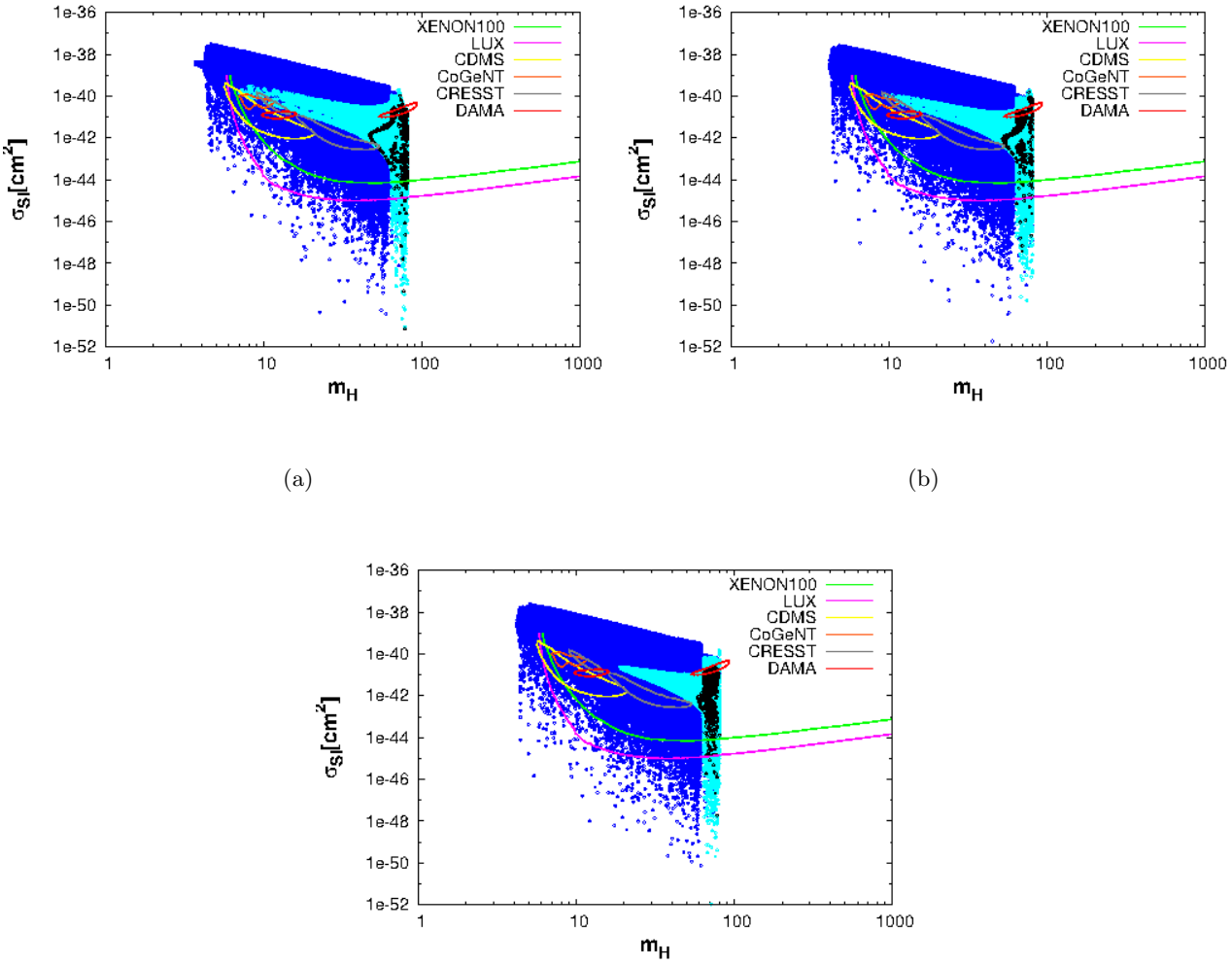

(a) (b)

(c)

Figure 3: Allowed regions in $m_H - \sigma_{SI}$ plane for $m_2 = 140, 150$ and 160 GeV.

$R_{\gamma\gamma}|_{\rm CMS} = 0.78$. It is therfore evident from Fig. 3(a-c) that imposition of signal strength ($R_{\gamma\gamma}$) results obtained from LHC, further constraints the allowed scattering cross-section limits obtained from direct detection experimental results for the DM candidate in our model. Investigating the region allowed by LUX and XENON experiments along with other direct dark matter experiments such as CDMS etc., it is evident from Fig. 3(a-c) that our model suggests a DM candidate within the range $m_1/2 < m_H < m_W$ GeV with scattering cross-section values $\sim 10^{-44} - 10^{-48}$ cm^2 with $m_1 = 125$ GeV, i.e., SM-like scalar. There are however few negligibly small allowed parameter space with $\sigma_{\rm SI}$ below $\sim 10^{-48}$ cm^2. It may also be noticed from Fig. 3 that the present model with all the constraints including $R_{\gamma\gamma}$ condition also partly agrees with allowed contour given by DAMA experiment. However, DAMA contour is ruled out

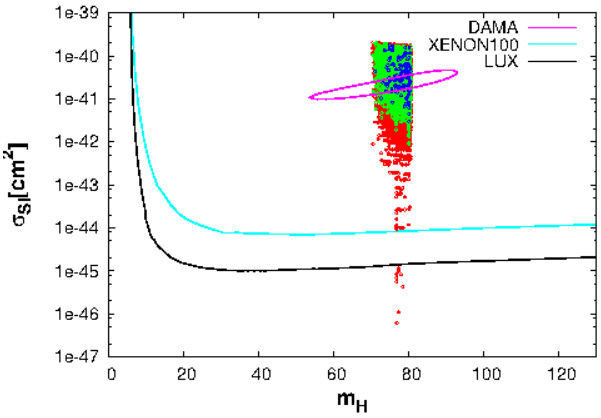

(a)

Figure 4: The m_H vs σ_{SI} parameter space for $R_{\gamma\gamma} \gtrsim 1$ for $m_2 = 140 - 160$ GeV.

by recent results from experiments like LUX and XENON100. Similar procedure has been adopted for restricting the $\sigma_{\rm SI} - m_H$ space with $R_{\gamma\gamma}$ limits from ATLAS experiment. In Fig. 4, the region shown in red corresponds to the region satisfying $R_{\gamma\gamma} \gtrsim 1$ with mass of h_2 varied from 140 GeV to 160 GeV. Also shown in Fig. 4, the scattered region in green (blue) represents the signal strength $R_{\gamma\gamma} = 1.65^{+0.34}_{-0.30}$ ($R_{\gamma\gamma} = 1.65$) as obtained from ATLAS experiment respectively. Fig. 4 shows that the part of the region constrained by ATLAS result is more stringent than that for CMS case and appears to satisfy only a part of DAMA allowed contour. There is however a negiligibly small allowed region satisfying the domain constrained by LUX or XENON100 expreiments. Similar to the case for $R_{\gamma\gamma}$ limit from CMS, here too, the allowed zone lies in the range around $m_H = 70$ GeV. Hence, in the present model H can serve as a potential dark matter candidate and future experiments with higher sensitivity like XENON1T [54], SuperCDMS [55] etc. are expected to constrain or rule out the viability of this model. In the present model we so far adopt the consideration that h_1 plays the role of SM Higgs and hence in our discussion we consider $h_1 \to \gamma\gamma$ for constraining our parameter space. The model considered in this work also provides us with a second scalar namely h_2. Since LHC has not yet observed a second scalar, it is likely that the other scalar h_2 is very weakly coupled to SM sector so that the corresponding branching ratios (signal strengths) are small. This may be justified in the present scenario if in case the $h_2 \to \gamma\gamma$ branching ratio or signal strength ($R'_{\gamma\gamma}$) is very small compared to that for h_1. Needless to mention that the couplings required to compute $R_{\gamma\gamma}$ and $R'_{\gamma\gamma}$ are restricted by dark matter constraints. One also has to verify whether the process $R'_{\gamma\gamma}$ can play significant role in restricting the dark matter model parameter space in the present framework. We address these issues by computing $R'_{\gamma\gamma}$ values and comparing them with $R_{\gamma\gamma}$ [4]. The computation of $R_{\gamma\gamma}$ and $R'_{\gamma\gamma}$ initially involves the dark matter model

[4]Since $R'_{\gamma\gamma}$ and $R'_{\gamma Z}$ are correlated, any suppression in $h_2 \to \gamma\gamma$ will be followed by similar effects in $h_2 \to \gamma Z$.

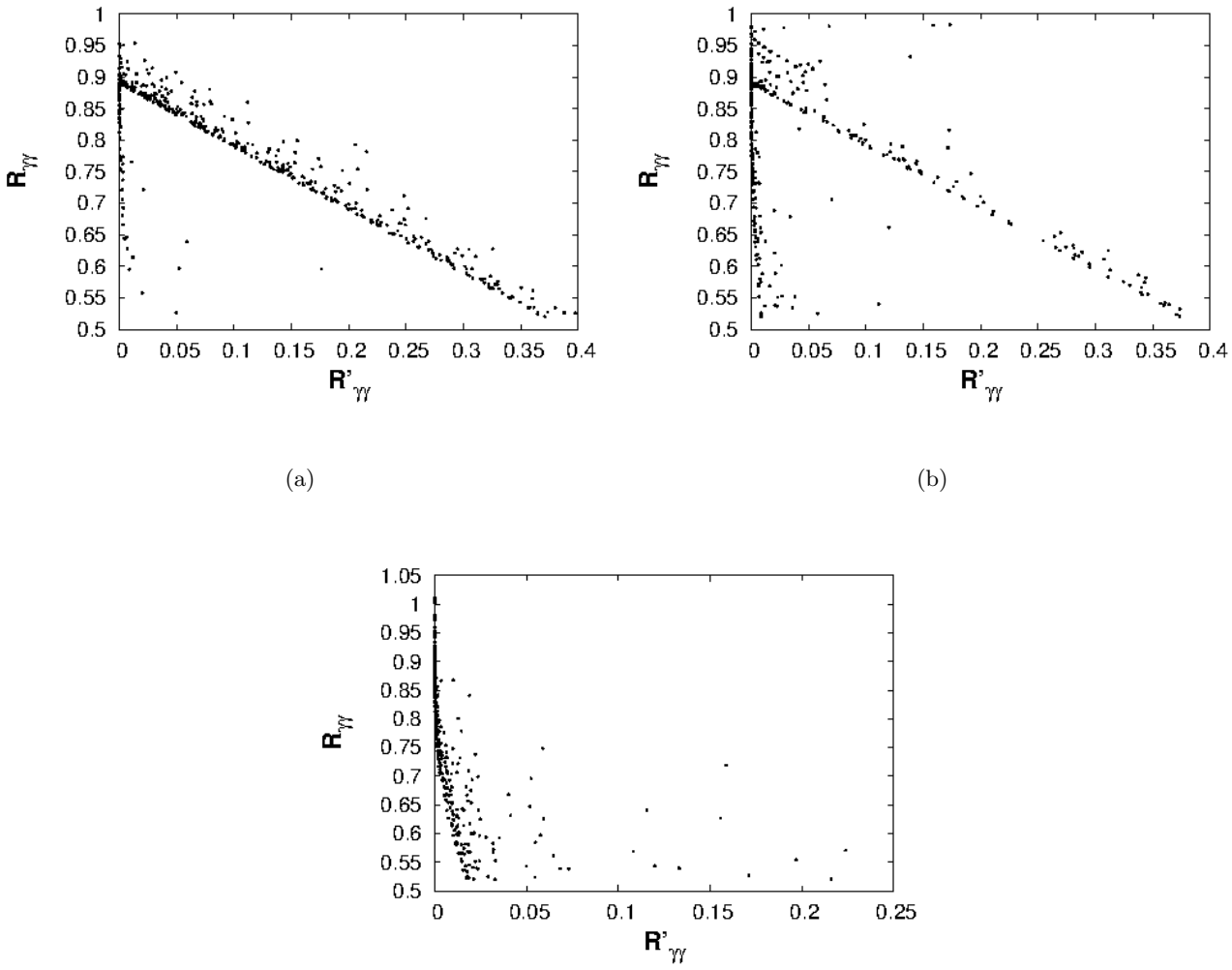

(a)

(b)

(c)

Figure 5: Allowed regions in $R_{\gamma\gamma} - R'_{\gamma\gamma}$ plane for $m_2 = 140, 150$ and 160 GeV.

parameter space that yields the dark matter relic density in agreement with PLANCK data as also the stringent direct detection cross-section bound obtained from LUX. $R_{\gamma\gamma}$ values thus obtained are not found to satisfy the experimental range given by ATLAS experiment. The resulting $R_{\gamma\gamma} - R'_{\gamma\gamma}$ is further restricted for those values of $R_{\gamma\gamma}$ which are within the limit of $R_{\gamma\gamma}|_{\rm CMS}$ given by CMS experiment. The region with black scattered points in Fig. 5(a-c) corresponds to the $R_{\gamma\gamma} - R'_{\gamma\gamma}$ space consistent with the model parameters that are allowed by DM relic density obtained from PLANCK, direct detection experiment bound from LUX and $R_{\gamma\gamma}|_{\rm CMS}$ for three different values of m_2 (140, 150, and 160 GeV). Fig. 5(a-c) reveals that $R'_{\gamma\gamma} \leq 0.4$ for $m_2 = 140,\ 150$ GeV whereas for $m_2 = 160$ GeV it is even less ($R'_{\gamma\gamma} < 0.25$) for $R_{\gamma\gamma}$ values compatible with CMS results. In Table 1 we further demonstrate that

m_2 in GeV	m_H in GeV	$m_{H^\pm}$ in GeV	α	$R_{\gamma\gamma}$	$R'_{\gamma\gamma}$	$Br(h_2 \to \gamma\gamma)$	σ_{SI} in cm^2
140.00	70.13	231.00	02	0.889	1.13e-03	1.835e-03	1.360e-47
	67.45	151.00	12	0.856	4.48e-05	2.038e-06	7.405e-48
	78.40	302.50	07	0.873	1.70e-02	2.256e-03	2.046e-46
150.0	64.05	181.00	20	0.786	3.50e-03	4.220e-05	6.386e-46
	79.57	242.50	04	0.889	2.63e-03	7.613e-04	5.749e-47
	80.29	138.00	10	0.875	3.67e-02	1.715e-03	8.437e-48
160.0	66.67	206.50	13	0.844	5.67e-05	6.217e-07	6.961e-50
	74.49	136.50	06	0.900	1.80e-07	9.165e-09	1.491e-47
	77.86	311.50	16	0.821	1.71e-03	1.255e-05	7.371e-49

Table 1: Benchmark points satisfying observed DM relic density obtained from PLANCK data and direct detection cross-section reported by LUX results for three different choices of h_2 mass.

within the framework of our proposed model for LIP dark matter, $R'_{\gamma\gamma}$ is indeed small compared to $R_{\gamma\gamma}$. We tabulate the values of both $R_{\gamma\gamma}$ and $R'_{\gamma\gamma}$ for some chosen values of LIP dark matter mass m_H. These numerical values are obtained from the computational results consistent with LUX direct DM search bound. Also given in Table 1 the corresponding mixing angles α between h_1 and h_2, the scalar masses $m_H^\pm$, h_2 to di-photon branching ratio and the scattering cross-section $\sigma_{\rm SI}$ for three different values of m_2 considered in the work. It is also evident from Table 1 that $R_{\gamma\gamma} >> R'_{\gamma\gamma}$ and mixing angles corresponding to respective values are small. In fact for some cases such as for $m_H = 70.13$ GeV ($m_2 = 140$ GeV) $R_{\gamma\gamma} = 0.889$ whereas $R'_{\gamma\gamma} \sim 10^{-3}$ and α is as small as 2. This demonstrates that the scalar h_1 in Eq. 4 is mostly dominated by SM-like Higgs component and the major component in the other scalar is the real scalar singlet s of the proposed model. Table 1 also exhibits that the signal strength $R'_{\gamma\gamma}$ for $h_2 \to \gamma\gamma$ channel is negligibly weak.

6 Summary

In this paper we have proposed a model for dark matter where we consider an extended two Higgs doublet model with an additional singlet scalar. The DM candidate follows by setting one of the Higgs doublet to be identical with an inert Higgs doublet imposing a Z_2 symmetry on the potential. This ensures the DM candidate that follows from the added inert doublet is stable. The inert doublet does not generate any VEV and hence cannot couple to Standard Model fermions directly. The scalar singlet, having no such discrete symmetry aquires a non zero VEV and mixes up with SM Higgs. The unknown couplings appearing in the model, which are basically the model parameters, are restricted

with theoretical and experimental bounds. The mixing of the SM and the singlet scalar gives rise to two sclar states namely h_1 and h_2. For small mixing h_1 behaves as the SM Higgs and h_2 as the added scalar. We extensively explored the scalar sector of the model and studied the signal streghts $R_{\gamma\gamma}$ and $R_{\gamma Z}$ for the SM- like Higgs (h_1) in the model. The range and region of enhancement depens on the mass of the singlet like scalar h_2. Appreciable enhancement of signals depends on h_2 mass which occurs near the Higgs resonance. Increase in signal strengths is not allowed for heavier values of h_2 mass. Enhancement of signals are forbidden when the invisible decay channel remains open. The extent of enhancement depends on the charged scalar mass and occurs only when the Higgs-charged scalar coupling $\lambda_{h_1 H^+ H^-} < 0$. We first restrict our parameter space by calculating the relic density of LIP dark matter in the framework of our model. Using the resultant paramter space obtained from relic density bounds we evalute the signal strengths $R_{\gamma\gamma}$ and $R_{\gamma Z}$ for different dark matter mass. We then restrict the parameter space by calculating the spin independent scattering cross-section and comparing it with the existing limits from ongoing direct detection experiments like CDMS, CoGeNT, DAMA, XENON100, LUX etc. Employing additional constraints by requiring that $R_{\gamma\gamma}$ and $R_{\gamma Z}$ will satisfy the CMS bounds and ATLAS bounds, we see that the present model not only provides a good DM candidate in middle mass region consistent with LUX and XENON100 bounds. The possibility that $R_{\gamma\gamma}(> 1.0)$ in the present framework does not seem to be favoured by LUX and XENON100 data. However, DAMA results appear to favour $R_{\gamma\gamma} \geq 1$. Therefore, we conclude that under the present framework, Inert Doublet Model with additional scalar singlet provide a viable DM candidate with mass range $m_1/2 < m_H < m_W$ GeV that not only is consistent with the direct detection experimental bounds and PLANCK results for relic density but also in agreement with the Higgs search results of LHC. A singlet like scalar that couples weakly with SM Higgs may also exist that could enrich the Higgs sector and may be probed in future collider experiments.

Acknowledgments : A.D.B. would like to thank A. Biswas, D. Das and K.P. Modak for useful discussions.

Appendix A

In Section 3.3 we have derived the decay widths $h_1 \to \gamma\gamma$ and $h_1 \to \gamma Z$ in terms of the loop factors $F_{1/2}$, F_1, F_0, $F'_{1/2}$, F'_1 and I_1 respectively. Factors $F_{1/2}$, F_1, F_0, for the measurement of $h_1 \to \gamma\gamma$ decay width can be written as [56, 57, 58]

$$\begin{aligned} F_{1/2}(\tau) &= 2\tau[1 + (1-\tau)f(\tau)], \\ F_1(\tau) &= -[2 + 3\tau + 3\tau(2-\tau)f(\tau)], \\ F_0(\tau) &= -\tau[1 - \tau f(\tau)], \end{aligned}$$

and

$$f(\tau) = \begin{cases} \arcsin^2\left(\frac{1}{\sqrt{\tau}}\right) & \text{for} \quad \tau \geq 1, \\ -\frac{1}{4}\left[\log\left(\frac{1+\sqrt{1-\tau}}{1-\sqrt{1-\tau}}\right) - i\pi\right]^2 & \text{for} \quad \tau < 1. \end{cases}$$

Loop factors for the decay $h_1 \to \gamma Z$ are expressed following Refs. [56, 57, 58]

$$\begin{aligned} F'_{1/2}(\tau,\lambda) &= I_1(\tau,\lambda) - I_2(\tau,\lambda), \\ F'_1(\tau,\lambda) &= c_W \left\{ 4\left(3 - \frac{s_W^2}{c_W^2}\right) I_2(\tau,\lambda) + \left[\left(1+\frac{2}{\tau}\right)\frac{s_W^2}{c_W^2} - \left(5+\frac{2}{\tau}\right)\right] I_1(\tau,\lambda) \right\}, \end{aligned}$$

where

$$\begin{aligned} I_1(a,b) &= \frac{ab}{2(a-b)} + \frac{a^2b^2}{2(a-b)^2}\left[f(a)-f(b)\right] + \frac{a^2 b}{(a-b)^2}\left[g(a)-g(b)\right], \\ I_2(a,b) &= -\frac{ab}{2(a-b)}\left[f(a)-f(b)\right]. \end{aligned}$$

Expressions of $g(\tau/\lambda)$ is given by

$$g(\tau) = \begin{cases} \sqrt{\tau-1}\arcsin\sqrt{\frac{1}{\tau}} & \text{for} \quad \tau \geq 1, \\ \frac{\sqrt{1-\tau}}{2}\left(\log\frac{1+\sqrt{1-\tau}}{1-\sqrt{1-\tau}} - i\pi\right) & \text{for} \quad \tau < 1. \end{cases}$$

References

[1] G. Aad *et al.* [ATLAS Collaboration], Phys. Lett. B **716**, 1 (2012).

[2] S. Chatrchyan *et al.* [CMS Collaboration], Phys. Lett. B **716**, 30 (2012).

[3] ATLAS-CONF-2013-012.

[4] CMS-HIG-13-001.

[5] P. Ade *et al.* [PLANCK Collaboration], arXiv:1303.5076 [astro-ph.CO].

[6] N. Jarosik, C. L. Bennett, J. Dunkley, B. Gold, M. R. Greason, M. Halpern, R. S. Hill and G. Hinshaw *et al.*, Astrophys. J. Suppl. **192**, 14 (2011) [arXiv:1001.4744 [astro-ph.CO]].

[7] K. Griest and M. Kamionkowski, Phys. Rept. **333**, 167 (2000).

[8] G. Bertone, D. Hooper and J. Silk, Phys. Rept. 405, 279 (2005).

[9] G. Jungman, M. Kamionkowski and K. Griest, Phys. Rept. **267**, 195 (1996).

[10] H. -C. Cheng, J. L. Feng and K. T. Matchev, Phys. Rev. Lett. **89**, 211301 (2002).

[11] V. Silveira and A. Zee, Phys. Lett. B **161**, 136 (1985).

[12] J. McDonald, Phys. Rev. D **50**, 3637 (1994) [hep-ph/0702143 [HEP-PH]].

[13] C. P. Burgess, M. Pospelov and T. ter Veldhuis, M. C. Bento, O. Bertolami, R. Rosenfeld and L. Teodoro, Phys. Rev. D **62**, 041302 (2000) [astro-ph/0003350].

[14] V. Barger, P. Langacker, M. McCaskey, M. J. Ramsey-Musolf and G. Shaughnessy. Phys. Rev. D **77**, 035005 (2008) [arXiv:0706.4311 [hep-ph]].

[15] S. Andreas, T. Hambye and M. H. G. Tytgat. JCAP **0810**, 034 (2008) [arXiv:0808.0255 [hep-ph]].

[16] C. E. Yaguna. JCAP **0903**, 003 (2009) [arXiv:0810.4267 [hep-ph]].

[17] X. -G. He, T. Li, X. -Q. Li, J. Tandean and H. -C. Tsai, Phys. Rev. D **79**, 023521 (2009) [arXiv:0811.0658 [hep-ph]].

[18] X. -G. He, T. Li, X. -Q. Li, J. Tandean and H. -C. Tsai, Phys. Lett. B **688**, 332 (2010) [arXiv:0912.4722 [hep-ph]].

[19] A. Bandyopadhyay, S. Chakraborty, A. Ghosal and D. Majumdar, JHEP **1011**, 065 (2010) [arXiv:1003.0809 [hep-ph]].

[20] S. Andreas, C. Arina, T. Hambye, F. -S. Ling and M. H. G. Tytgat, Phys. Rev. D **82**, 043522 (2010) [arXiv:1003.2595 [hep-ph]].

[21] Y. Mambrini, Phys. Rev. D **84**, 115017 (2011) [arXiv:1108.0671 [hep-ph]].

[22] A. Biswas and D. Majumdar, Pramana **80**, 539 (2013) [arXiv:1102.3024 [hep-ph]].

[23] Y. G. Kim, K. Y. Lee and S. Shin, JHEP **0805**, 100 (2008) [arXiv:0803.2932 [hep-ph]].

[24] M. M. Ettefaghi and R. Moazzemi, JCAP **1302**, 048 (2013) [arXiv:1301.4892 [hep-ph]].

[25] M. Fairbairn and R. Hogan, JHEP **1309**, 022(2013) [arXiv:1305.3452 [hep-ph]].

[26] M. Aoki, S. Kanemura and O. Seto, Phys. Lett. B **685**, 313 (2010).

[27] Y. Cai, X.G. He, and B. Ren, Phys. Rev. D **83**, 083524 (2011) [arXiv:1102.1522 [hep-ph]].

[28] E. Ma, Phys. Rev. D **73**, 077301 (2006) [hep-ph/0601225].

[29] L. Lopez Honorez, E. Nezri, J. F. Oliver and M. H. G. Tytgat, JCAP **0702**, 028 (2007) [hep-ph/0612275].

[30] D. Majumdar and A. Ghosal, Mod. Phys. Lett. A **23**, 2011 (2008) [hep-ph/0607067].

[31] M. Gustafsson, E. Lundstrom, L. Bergstrom and J. Edsjo, Phys. Rev. Lett. **99**, 041301 (2007) [astro-ph/0703512].

[32] Q. -H. Cao, E. Ma and G. Rajasekaran, Phys. Rev. D **76**, 095011 (2007) [arXiv:0708.2939 [hep-ph]].

[33] E. Lundstrom, M. Gustafsson and J. Edsjo, Phys. Rev. D **79**, 035013 (2009) [arXiv:0810.3924 [hep-ph]].

[34] S. Andreas, M. H. G. Tytgat and Q. Swillens, JCAP **0904**, 004 (2009) [arXiv:0901.1750 [hep-ph]].

[35] L. Lopez Honorez and C. E. Yaguna, JHEP **1009**, 046 (2010) [arXiv:1003.3125 [hep-ph]].

[36] L. Lopez Honorez and C. E. Yaguna, JCAP **1101**, 002 (2011) [arXiv:1011.1411 [hep-ph]].

[37] D. Borah and J. M. Cline, Phys. Rev. D **86**, 055001 (2012) [arXiv:1204.4722 [hep-ph]].

[38] E. Aprile *et al.* [XENON100 Collaboration], Phys. Rev. Lett. **109**, 181301 (2012) [arXiv:1207.5988 [astro-ph.CO]].

[39] D. S. Akerib *et al.* [LUX Collaboration], arXiv:1310.8214 [astro-ph.CO].

[40] R. Agnese *et al.* [CDMS Collaboration], Phys. Rev. D **88**, 031104 (2013) [arXiv:1304.3706 [astro-ph.CO]]; R. Agnese *et al.* [CDMS Collaboration], [arXiv:1304.4279 [hep-ex]].

[41] R. Bernabei *et al.* [DAMA Collaboration], Eur. Phys. J. C **56**, 333 (2008) [arXiv:0804.2741 [astro-ph]]; R. Bernabei *et al.* [DAMA and LIBRA Collaborations], Eur. Phys. J. C **67**, 39 (2010) [arXiv:1002.1028 [astro-ph.GA]].

[42] C.E. Aalseth *et al.* [CoGeNT collaboration], Phys. Rev. Lett. **106**, 131301 (2011).

[43] G. Angloher, M. Bauer, I. Bavykina, A. Bento, C. Bucci, C. Ciemniak, G. Deuter and F. von Feilitzsch *et al.*, Eur. Phys. J. C **72**, 1971 (2012) [arXiv:1109.0702 [astro-ph.CO]].

[44] J. Beringer et al. (Particle Data Group), Phys. Rev. D **86** (2012) 010001.

[45] E.W. Kolb and M. Turner, *The Early Universe* (Westview Press, Boulder, 1990).

[46] A. Arhrib, R. Benbrik, and N. Gaur, Phys.Rev. D **85**, 095021 (2012), [arXiv:1201.2644 [hep-ph]].

[47] B. Swiezewska and M. Krawczyk, Phys. Rev. D **88**, 035019 (2013) [arXiv:1212.4100 [hep-ph]].

[48] A. Goudelis, B. Herrmann and O. Stal, JHEP **1309**, 106 (2013) [arXiv:1303.3010 [hep-ph]].

[49] P. Posch, Phys.Lett. B **696**, 447 (2011), [arXiv:1001.1759 [hep-ph]].

[50] G. Bhattacharyya, D. Das, P. B. Pal and M. N. Rebelo, JHEP **1310**, 081 (2013) [arXiv:1308.4297 [hep-ph]].

[51] A. Biswas, D. Majumdar, A. Sil, and P. Bhattacharjee, JCAP **1312**, 049 (2013) [arXiv:1301.3668 [hep-ph]].

[52] A. Denner et al.,Eur. Phys. J. C **71**, 1753 (2011) [arXiv:1107.5909 [hep-ph]].

[53] R. Barbieri, L. J. Hall and V. S. Rychkov, Phys. Rev. D **74**, 015007 (2006) [hep-ph/0603188].

[54] E. Aprile [XENON1T Collaboration], arXiv:1206.6288 [astro-ph.IM].

[55] R. Agnese et al. [SuperCDMS Collaboration], [arXiv:1402.7137 [hep-ex]].

[56] J. F. Gunion, H. E. Haber, G. L. Kane, and S. Dawson, Front. Phys. **80** 1 (2000).

[57] A. Djouadi, Phys. Rept. **459** (2008) 1 [arXiv:hep-ph/0503173].

[58] A. Djouadi, Phys. Rept. **457** (2008) 1 [arXiv:hep-ph/0503172].